

In-plane structure and ordering at liquid sodium surfaces and interfaces from *ab initio* molecular dynamics

Brent G. Walker

*Industrial Research Limited, 69 Gracefield Road,
P. O. Box 31-310, Lower Hutt 5040, New Zealand.**

Nicola Marzari

*Department of Materials Science and Engineering,
Massachusetts Institute of Technology, Cambridge, MA 02139, USA.*

Carla Molteni

*Physics Department, King's College London,
Strand, London, WC2R 2LS, UK.*

Abstract

Atoms at liquid metal surfaces are known to form layers parallel to the surface. We analyze the two-dimensional arrangement of atoms within such layers at the surface of liquid sodium, using *ab initio* molecular dynamics (MD) simulations based on density functional theory. Nearest neighbor distributions at the surface indicate mostly 5-fold coordination, though there are noticeable fractions of 4-fold and 6-fold coordinated atoms. Bond angle distributions suggest a movement toward the angles corresponding to a six-fold coordinated hexagonal arrangement of the atoms as the temperature is decreased towards the solidification point. We rationalize these results with a distorted hexagonal order at the surface, showing a mixture of regions of five and six-fold coordination. The liquid surface results are compared with classical MD simulations of the liquid surface, with similar effects appearing, and with *ab initio* MD simulations for a model solid-liquid interface, where a pronounced shift towards hexagonal ordering is observed as the temperature is lowered.

PACS numbers: 71.15.Mb, 71.15.Nc, 71.15.Pd, 73

Keywords: liquid metal surface, 2D order, surface-induced layering, *ab initio* molecular dynamics, density functional theory

I. INTRODUCTION

For a number of years there has been significant interest, from the theoretical^{3,4,5,6,7,8,9,10,11,12,13,14,16,17,18,19,37,44,48,52,53,54,55} and experimental^{1,20,22,23,24,25,26,29,31,32,33,34,35,39,41,45,46,47} points of view, in understanding liquid metal surfaces. This body of work has established that free liquid metal surfaces exhibit *surface-induced layering*, in which the liquid atoms near the surface form into layers parallel to it. This behavior does not generally occur at free surfaces of liquid dielectrics – though it is well known that atomic layers form at the solid-liquid interfaces of both dielectric and metallic substances³⁸ due to geometrical confinement. Surface-induced layering at free liquid metal surfaces was predicted theoretically^{7,8,9,10,16,17,18,37}, and subsequently confirmed experimentally^{20,26,29,31,32,33,34,35,39,46,47} for various metals and alloys by x-ray reflectivity measurements. An understanding of the behavior of liquid metal surfaces is important for instance to recent studies of studying nanoscale metal alloy droplets⁴³.

In addition to providing various hypotheses for the mechanism of layer formation, simulations have also led to suggestions regarding the existence of two-dimensional order within the layers. In glue model simulations of super-cooled liquid Au surfaces, evidence was found by Celestini *et al*³ for in-plane order with mostly six-fold coordinated sites, interspersed with five-fold and seven-fold coordinated ones, in the plane of the surface. They claimed that a transition to a true hexatic phase², in which each atom is on average six-fold coordinated, is preempted by solidification of the system. Also of relevance to ordering within the layers is the experimental work by Reichert *et al*³⁶ on liquid Pb in contact with a solid Si substrate; lead atoms arranged as fragments of icosahedra were observed to be attached to the substrate, meaning that the Pb atoms were five-fold coordinated at that interface. A similar atomic arrangement might be seen near the free surface of a liquid metal if the rapid decay of the electronic density there acts as a hard wall against which the atoms pack (as in the suggestion by Rice *et al* for the mechanism of layer formation^{5,6,7,8,9,10,12,16,17,18,37,52,53,54,55}, and supported by our simulations^{49,50}, that makes the analogy with the formation of atomic layers at solid-liquid interfaces). In addition, it has been proposed that the natural arrangement of Pb atoms in the bulk liquid is as icosahedra⁴². So far however no experimental evidence has been found for in-plane ordering at free liquid metal surfaces, though investigations using grazing incidence x-ray techniques are ongoing^{1,40}.

We study in detail the properties of free liquid metal surfaces with extensive *ab initio* molecular dynamics (MD) simulations of the free liquid surface of sodium. These simulations are made using the Born-Oppenheimer MD scheme, with the forces acting on the atoms at each timestep of the dynamics determined via a first principles electronic structure calculation. The ensemble density functional theory and the cold-smearing generalized entropy function²⁷, with plane wave basis sets and norm-conserving pseudopotentials, are employed to determine the electronic structure at each timestep of the MD. This methodology has been demonstrated to be particularly efficient for studying dynamical properties of metallic systems^{28,30}. Slab geometries, with periodic boundary conditions, are used to model the free surfaces, making use of unit cells with two different cross-sectional shapes parallel to the surface. These two types of cell, labeled “(001)” and “(111)”, containing 160 and 162 atoms respectively, are obtained by taking the solid bcc sodium crystal viewed along either the (001) or (111) directions, melting these as bulk systems (so there is no vacuum region or surface in each case), and finally adding large vacuum regions (of ~ 11 Å thickness) to form liquid slabs, each having two surfaces. Each of the two cell geometries is simulated at two temperatures ($T = 400$ K and $T = 500$ K) above the melting temperature of sodium ($T_M = 373$ K), meaning a total of four *ab initio* simulations of the free liquid surface are undertaken. The use of simulation cells with different cross-sectional shapes parallel to the surface allows assessment of whether the cross-sectional geometry has an effect on any in-plane ordering that might be seen; for instance, it may be that a particular shape is more or less consistent with a certain type of atomic arrangement parallel to the surface. Long simulations (>50 ps) are made for each of the two cell shapes at each of the two temperatures. In each free liquid surface simulation the last 30 ps of the MD run is used for determination of time-averaged properties.

These dynamical simulations provide detailed microscopic information from which various properties related to the arrangements of the atoms at the surface can be extracted. Full details of the MD simulations are laid out in Refs. 49 and 50, where we concentrate on understanding the mechanism of layer formation, in particular with respect to the relevance of Friedel oscillations and geometrical confinement effects at free liquid metal surfaces, and the spacing and structure of the layers normal to the surface.

In the present paper we focus on the two-dimensional atomic arrangements *within* the layers formed at the liquid sodium surface. We complement the *ab initio* MD simulations of

the free liquid surface with classical MD simulations of the free liquid surface, and *ab initio* MD simulations of a model of the solid-liquid interface.

II. RESULTS AND DISCUSSION

A. *Ab initio* MD liquid surface simulations

The atomic arrangements parallel to the surface are considered firstly by looking at density profiles along the surface normal. These exhibit clear oscillations at the surface, indicating surface-induced layering. In all our *ab initio* free surface simulations (where the systems contain ~ 160 atoms), 7 layers are formed⁴⁹. While the presence of layers throughout the slabs is due to their limited sizes, we have demonstrated⁴⁹ that the layered structures of the two surfaces in each case are independent of one other.

To examine the atomic structure within the surface layers – our primary concern here – we determine a number of properties: pair correlation functions, nearest neighbor distributions, bond angle distributions and two-dimensional density plots in planes parallel to the surface. The parts of the slabs considered as the surface layers, the 2nd surface layers and the inner regions for calculating these various properties are illustrated in Fig. 1 by way of one of the transverse density profiles (that obtained for the (001) cell) at $T = 400$ K): we emphasize that we take the surface layers to be those regions on either side of the slab beyond the first minimum in the density profile.

Transverse atomic pair correlation functions^{5,18,53,54,55} for the surface layers, the 2nd surface layers, and slices within the bulk regions appear in Fig. 2. In comparing the correlation functions in the surface layers with those for the 2nd surface layers and the inner parts of the slabs (obtained by averaging over *all* the inner layers), we see that the positions of the first peaks are all essentially the same. In all cases however, there is an observable shift of the second peak to larger values (of $\sim 3\%$) at the surface. The 2nd surface layers and the inner regions have coincident pair correlation functions. This shift in the second peak in the correlation functions at the surface indicates that the *second* coordination shell is less tightly packed at the surface than in the 2nd surface layers and the inner regions. The shifts observed in the peaks corresponding to the second coordination shell are consistent with the behavior observed in the orbital free DFT results of Ref. 15; however we note that in Ref. 15

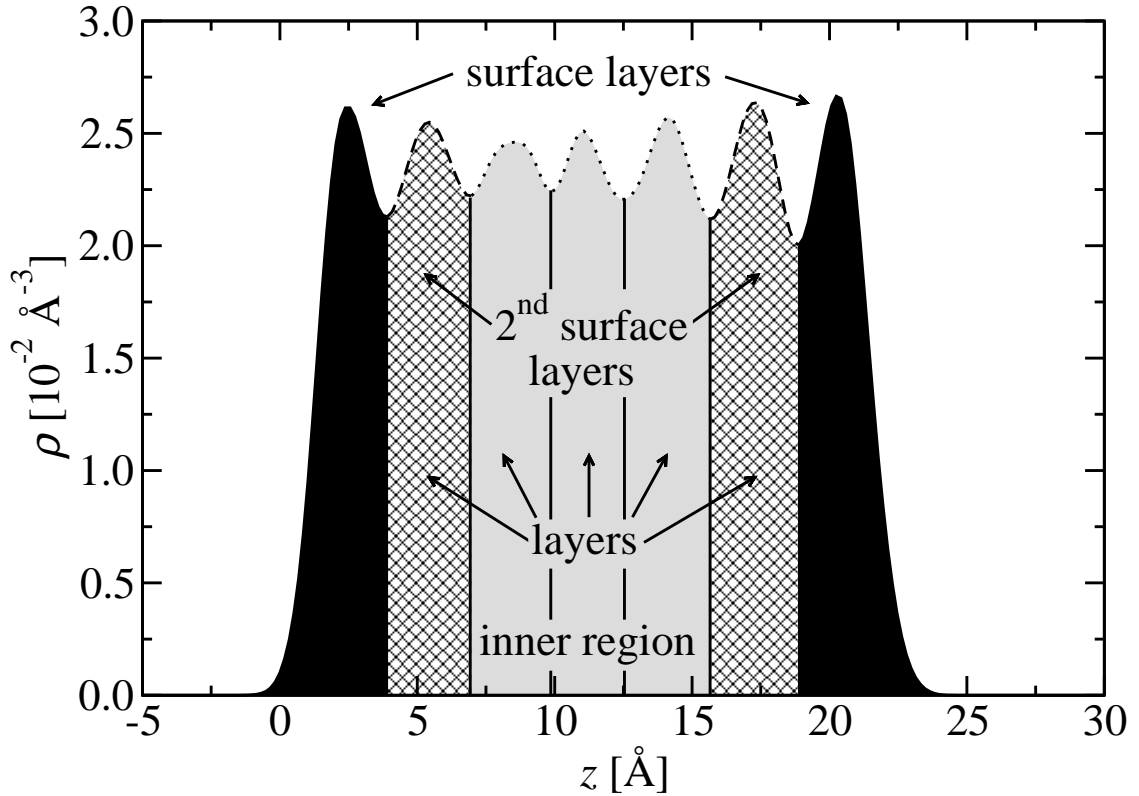


FIG. 1: Density profile through slab [(001) cell, $T = 400$ K] illustrating the regions considered as surface layers (black), 2nd surface layers (hashed) and inner (grey) for calculation of pair correlation functions, and bond angle and nearest neighbor distributions.

shifts toward larger radii are also seen in the peaks corresponding to the *first* coordination shells for Na and Li, that we do not observe in our *ab initio* free surface simulations. The most probable nearest neighbor distance, calculated as the average position of the first peak in the pair correlation function is $r_{\text{nn}} = 3.8 \text{ \AA}$.

For comparison, the transverse pair correlation functions averaged over a number of slices of similar thickness to the surface regions are compared with the three-dimensional bulk pair correlation function for all of the inner region in Fig. 3. It is clear that they coincide, meaning that the differences in the transverse correlation function at the surface and in the inner regions are genuinely due to differences in atomic arrangements at the surface.

In Fig. 4 we show the nearest neighbor distributions obtained from the surface simulations. These were calculated by counting for each atom the number of atoms within a sphere of a chosen radius centered on that atom; for the radius of this “nearest neighbor” sphere,

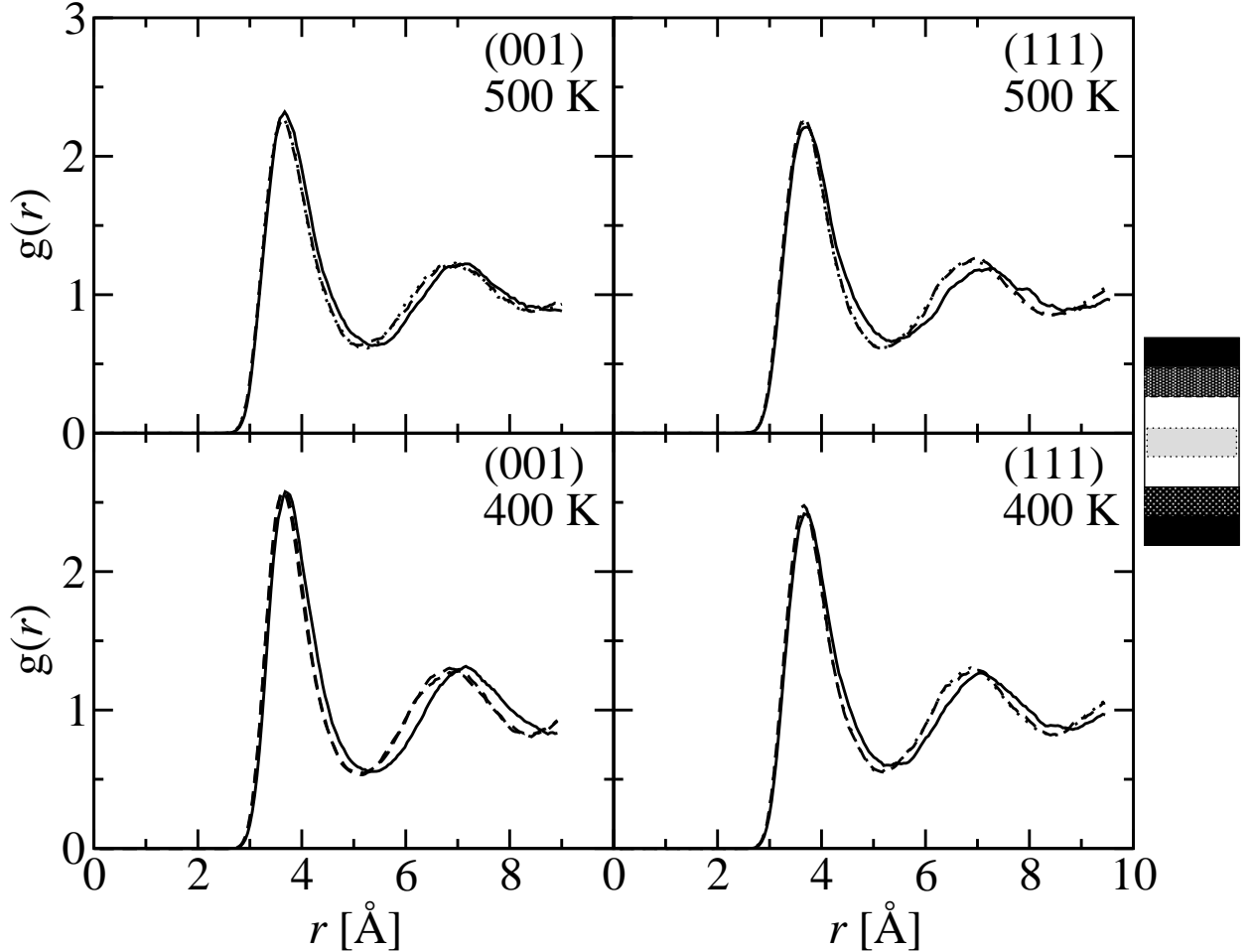


FIG. 2: Transverse atomic pair correlation functions for sodium from *ab initio* MD surface simulations. Solid lines: averaged over surface layers; dashed lines: averaged over 2nd surface layers; dotted lines: averaged over layers in the inner regions. The bar at the right indicates the regions of the simulation slabs considered in each case.

we used the value $r_{\text{cut}} = 5.32 \text{ \AA}$, which is the position of the first minimum in the bulk liquid pair correlation function. Reasonable variations in the value used for the radius of the nearest neighbor sphere do not in fact observably affect the nearest neighbor distributions (the value used is a sensible choice, lying roughly midway between the first minima in the surface and inner transverse pair correlation functions shown in Fig. 2).

The majority of atoms in the surface layer have 5 neighbors, though there are significant fractions ($\sim 30\%$) with coordination numbers of 4 and 6 (the latter accounting for the higher fraction of the two). When the temperature is lowered, the percentage of 4-fold coordinated

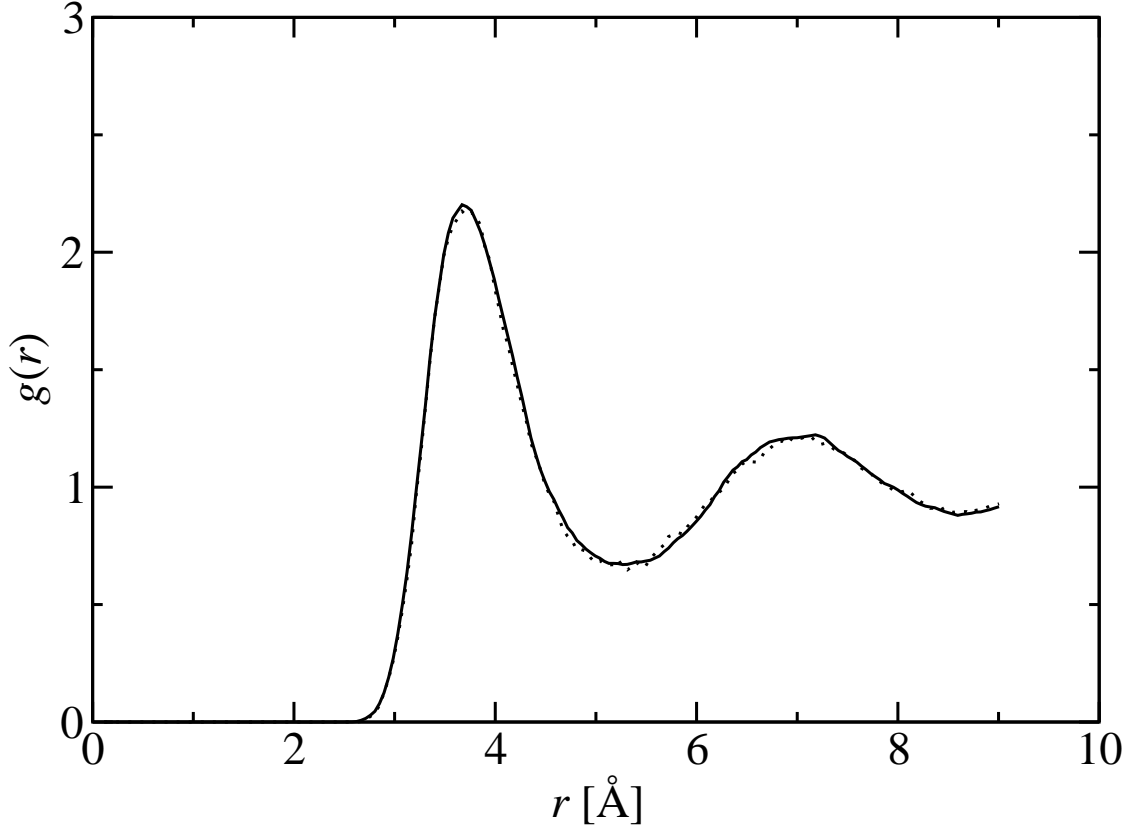


FIG. 3: Comparison between the three-dimensional pair correlation function calculated in the inner region of the slabs (solid curve) and the average transverse pair correlation function for slices of comparable thickness to the surface regions, calculated within the inner region (dotted curve). The data refers to the (001) simulation cell at $T = 500$ K.

atoms decreases, and the percentages of atoms 5 and 6-fold coordinated increase. This is consistent with the presence of *icosahedral* fragments, in which each atom is 5-fold coordinated (as seen in the experimental studies of liquid Pb in contact with solid Si³⁶, and in line with the suggested arrangement of atoms in the bulk liquid metals as icosahedra⁴²), mixed with 6-fold coordinated regions (as suggested by Celestini *et al*³), the latter regions becoming larger as the temperature is lowered and correspondingly the disorder is reduced. Coordination numbers obtained from the nearest neighbor distributions are shown in Table I and are generally just over 5 for the surface regions of Fig. 1.

These average coordination numbers are significantly less than the value of $n_c^{\text{bulk}} = 13.14$ obtained from a 500 K bulk liquid simulation we performed using the same DFT MD methodology. This is around the value of 13 typical of a bulk liquid, and in agreement with the

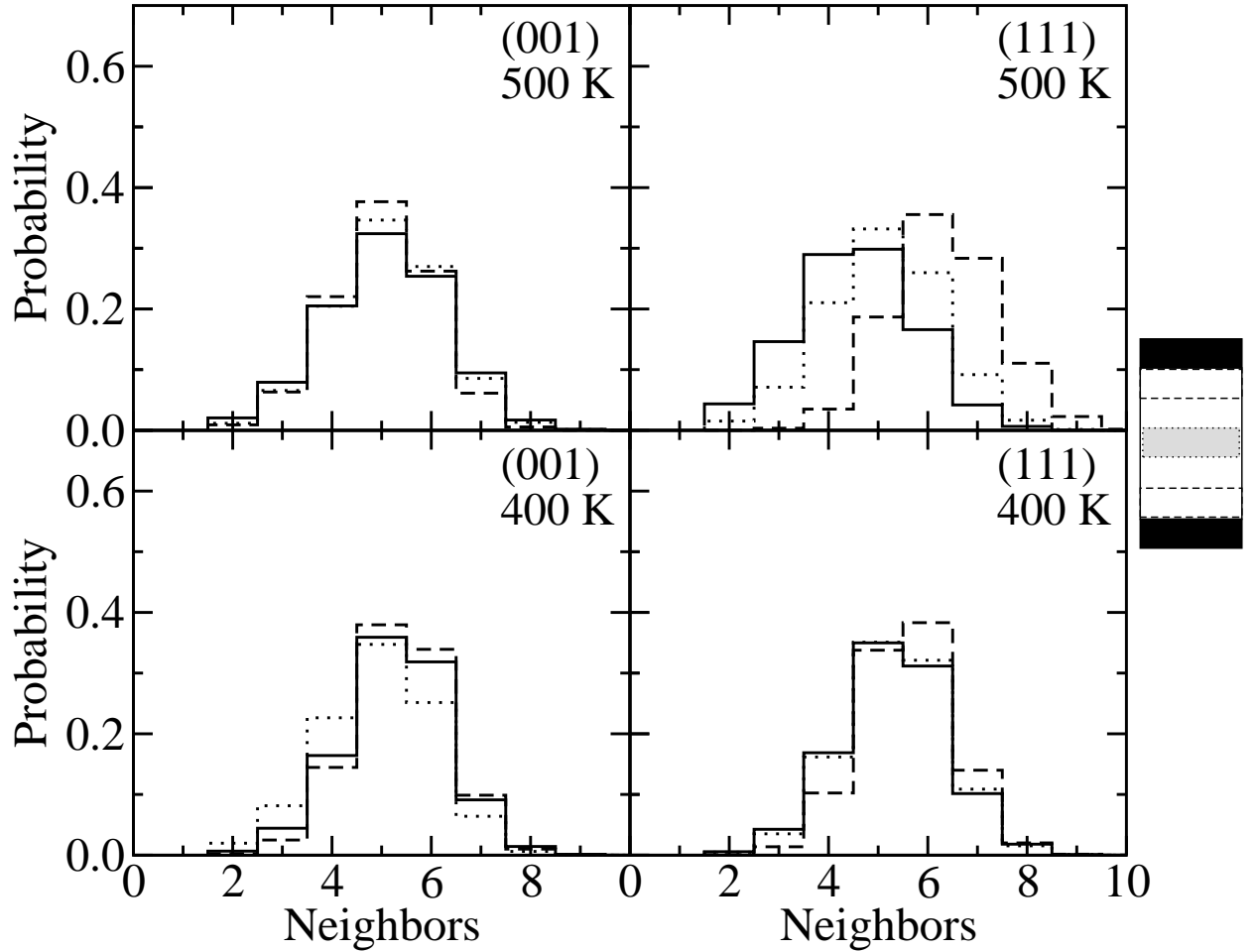


FIG. 4: Nearest neighbor distributions from *ab initio* slab simulations. Solid profiles: surface layers; dashed profiles: 2nd surface layers; dotted profiles: layers in inner region.

T [K]	Surface Layer		2nd Surface Layer		Inner	
	(001)	(111)	(001)	(111)	(001)	(111)
400	5.3	5.3	5.5	5.6	4.9	5.3
500	5.1	4.5	5.0	6.3	5.1	5.1

TABLE I: Coordination numbers n_c obtained by averaging nearest neighbor distributions shown in Fig. 4.

value of 13 obtained for Na in earlier bulk sodium calculations²¹.

We note that the (111), $T = 500$ K density profile is less than ideally symmetric, and this has something of an adverse effect on the other properties determined for that simulation.

Bond angle distributions for the slabs appear in Fig. 5. There we compare the distributions of angles for the surface layers, the 2nd surface layers, and for layers in the interior of the slab. The distributions are calculated using the same nearest neighbor sphere as considered in determining the nearest neighbor distributions. To calculate the bond angle distributions, the bond angles between an atom and each pair of other atoms lying within the nearest neighbor sphere centered on the first atom are determined. In general, comparing the surface layer, 2nd surface layer and inner bond angle distributions shows there to be little difference between the bond angle distributions in the different regions of the slabs at the same temperature. In comparing the bond angle distributions at the different temperatures, the separation of a small shoulder at large angles can be seen at the lower temperature. This may signal an enhancement of the angles (60° , 120° and 180°), the three bond angles characteristic of six-fold coordinated hexagonal ordering. However, it should be noted that the bond angles that would appear in an icosahedral fragment are 63.5° and 116.5° , so it is difficult to say whether the fairly small changes seen here in the bond angle indicate strengthening of 5 or 6-fold ordering.

If attention is confined to small regions located right at the outermost peaks (as illustrated in Fig. 6), the movement of concentration towards the angles 60° , 120° and 180° becomes more pronounced, as shown in Fig. 7.

When we restrict attention to the narrow regions centered on the outermost (surface) peaks, the quality of the statistics is correspondingly lowered. Here finite size effects in the statistics are clearly much more important, as can be seen easily from the level of noise in the bond angle distributions found in the “peak” regions.

B. Classical MD liquid surface simulations

To complement the *ab initio* simulation results, we also perform explorations using classical MD simulations. Because the statistics that can be collected with the (less accurate) classical simulations are much longer than those obtainable with *ab initio* MD, classical MD provides us with a convenient check on simulation time effects in the statistics (also larger numbers of atoms can be simulated with classical simulations).

The classical surface samples were obtained – in analogy with the *ab initio* setup procedure – by melting a crystal lattice at high temperature, followed by addition of a vacuum

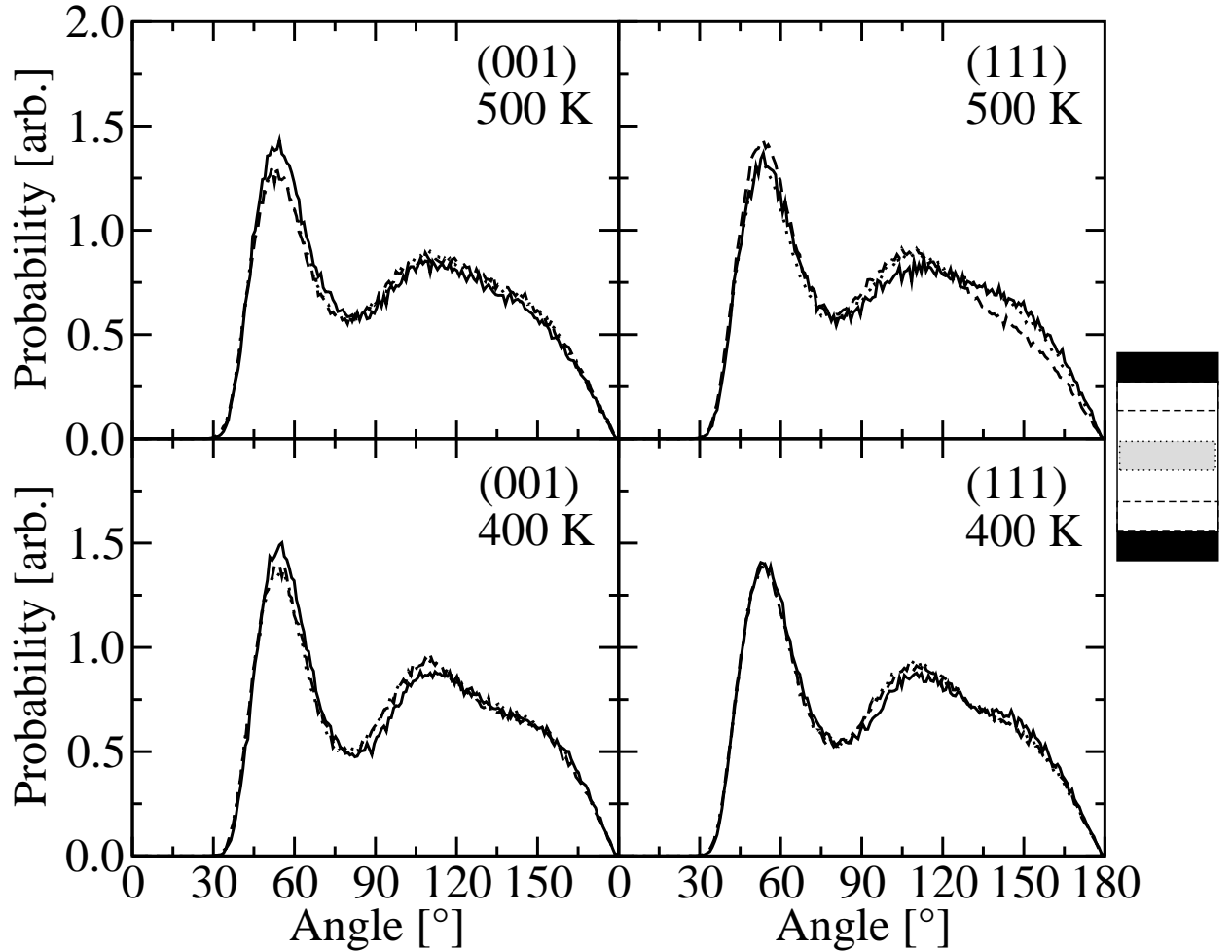


FIG. 5: Bond angle distributions calculated in various slices of the *ab initio* MD slabs. Solid curves: surface layers; dashed curves: 2nd surface layers; dotted curves: averages over the inner layers.

region of thickness ~ 11 Å along the z direction to form a slab of atoms, and equilibration at the temperatures of interest. The cells have the same shape as the (001) cells used in the *ab initio* simulations, but are larger, containing 720 atoms (the atomic slabs are roughly twice as thick as in the *ab initio* simulations and are about 20 % larger in each of the transverse directions; the corresponding solid slab would contain 20 layers parallel to the surfaces, and 12 layers in the x and y directions). The length of time simulated was roughly 10 times that achieved in the *ab initio* surface simulations. The potential used to model the interactions between the atoms in the classical simulations was that fitted for sodium by Chacón *et al*^{4,44,48,49,50}.

In Fig. 8 we plot the pair correlation functions, nearest neighbor distributions, and bond

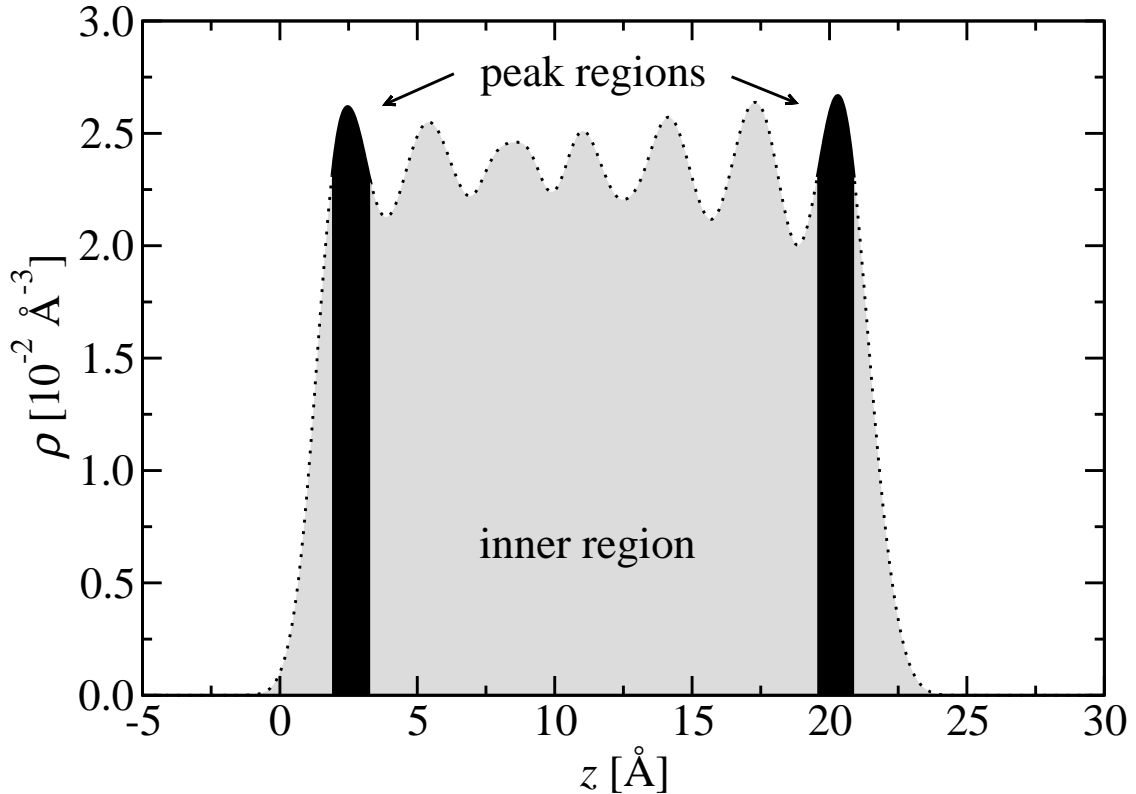


FIG. 6: Illustration of the “peak” regions (black).

angle distributions for classical simulations at temperatures $T = 550$ K, $T = 600$ K, $T = 650$ K, $T = 700$ K (the melting temperature for the pair potential is approximately $T = 650$ K). To obtain the averages over the inner regions of the slabs we have used the discernible layers in going from the surface into the slab; as the slabs in the classical simulations are twice as thick as those in the *ab initio* simulations, there are regions in the centers where a layered structure is not clear, that is, the bulk liquid limit has been reached in those regions.

The pair correlation functions obtained from our classical surface simulations show – in addition to shifts in the positions of the second peaks to larger radii – shifts in the *first* peaks to larger radii in the outermost surface layer, with there being very little difference between the profiles in the 2nd surface layers and those in the inner layers. The shifts in the first peaks are consistent with the behavior seen in the profiles for sodium shown in Fig. 7 of Ref. 15, though the shifts we see in the first peak are larger than theirs; this is however different from the behavior seen in our *ab initio* free surface simulations (cf. Fig. 2).

The nearest neighbor distributions are centered on 5, and most atoms have 5 nearest

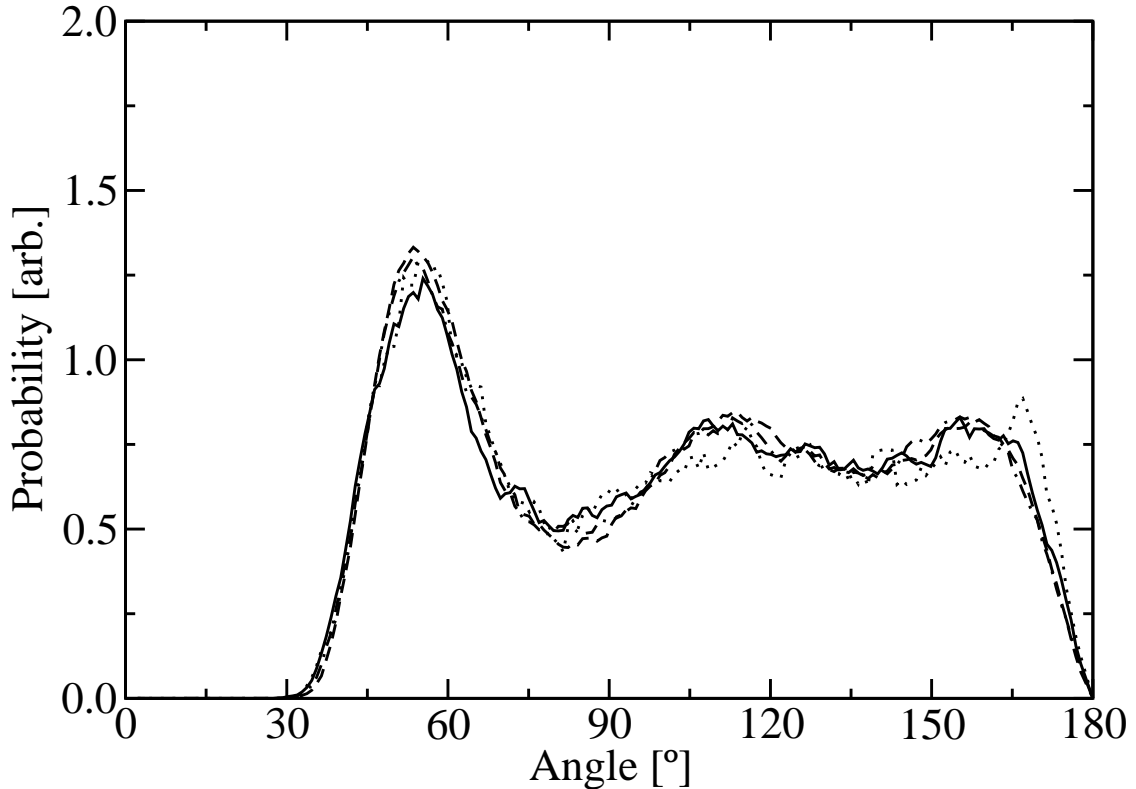


FIG. 7: Bond angle distributions calculated in the peak regions illustrated in Fig. 6 for *ab initio* free surface simulations. The curves refer to the simulations as follows: solid: (001), $T = 500$ K; dotted: (111), $T = 500$ K; dashed: (001), $T = 400$ K; dot-dashed: (111), $T = 400$ K.

neighbors, though there are significant fractions of atoms having coordination numbers of 4 and 6. At the surface, the nearest neighbor distributions are shifted towards lower coordination. As the temperature is reduced, the distribution – still centered on 5 – becomes slightly narrower, suggesting the degree of order is increased. The average coordination numbers obtained by averaging the nearest neighbor distributions are shown in Table II.

The classical simulation coordination numbers are significantly smaller for the surface layers than the second surface and inner layers. Much smaller differences are seen between the coordination numbers in the second surface layers and the inner layers. Notably, the differences between the surface layer and the second surface and inner layers in the classical simulations are greater than in the *ab initio* simulations, though comparable to the differences between the surface, second surface and inner layers presented in Table IV of Ref. 15. This is reminiscent of the density profiles normal to the surface⁴⁹, in that the density pro-

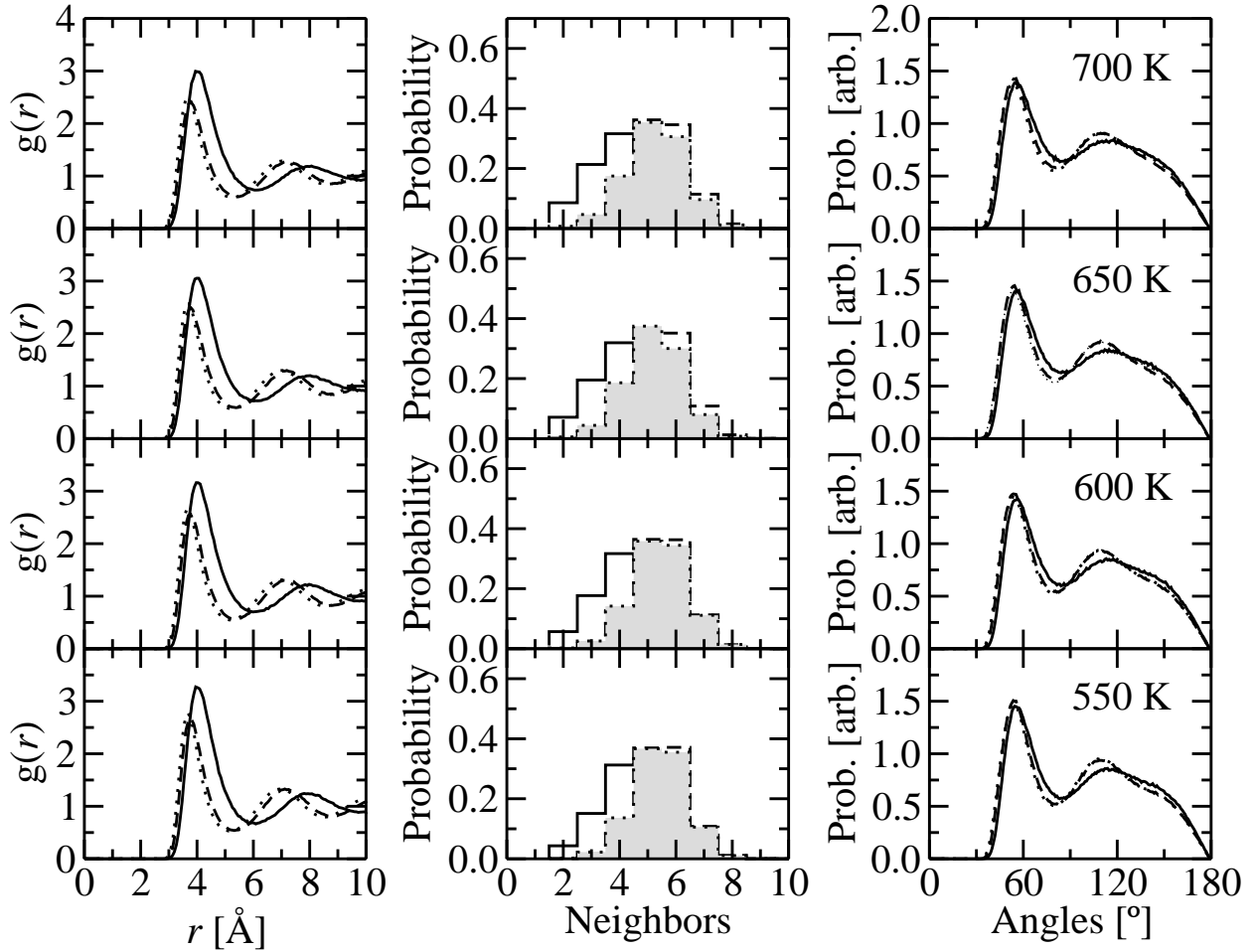


FIG. 8: Transverse pair correlation functions (left panels), nearest neighbor distributions (middle panels), and bond angle distributions (right panels) calculated for classical MD surface simulations. The temperatures are, from top to bottom: 700 K, 650 K, 600 K, and 550 K. In all cases, solid profiles refer to the surface layers, dashed profiles to the 2nd surface layers, and dotted profiles to averages over the inner layers.

files in the classical simulations were qualitatively the same as those in Ref. 15 – with the surface peak significantly lower in height than the 2nd surface peak and the inner peaks – in contrast to the density profiles seen in our *ab initio* simulations, where the outermost peaks were at roughly the same heights as the second surface and inner peaks. Additionally, we see decreases in the coordination numbers in the surface layers, the second surface layers, and the inner layers as the temperature is increased in the classical simulations.

The bond angle distributions show the same sort of behavior as observed in the *ab initio*

T [K]	Surface Layer	2nd Surface Layer	Inner
550	4.4	5.5	5.4
600	4.3	5.5	5.4
650	4.2	5.4	5.2
700	4.1	5.4	5.2

TABLE II: Coordination numbers n_c obtained by averaging nearest neighbor distributions from the classical simulations shown in Fig. 8.

free surface simulations, that is, the separation of shoulders in the distributions in the surface layer. Here it is clear that the bond angle distributions in the 2nd surface layer and the inner layers coincide, and there is a difference between the surface layer and the second surface and inner layers. The change in the bond angle distributions at the surface suggests more convincingly a movement of weight towards the angles consistent with 6-fold coordination.

C. *Ab initio* MD liquid-solid interface simulations

In addition to simulating the free liquid surface, we also consider MD simulations of a model representing the solid-liquid interface, constructed by placing a close-packed layer of fixed atoms within a bulk cell. A random time step from a well-equilibrated $T = 500$ K bulk liquid *ab initio* MD simulation is taken, and 24 of the atoms are placed onto the plane $z = 0$ in a distorted hexagonal 2D arrangement (this is dictated by the use of a cell with a square planar cross-section). Our initial motivation for constructing such a model was that for sodium the electronic charge density will be almost continuous normal to the “interface” (that is, there would be no rapid decrease in the electronic density as there is at the free liquid surface), allowing us to cleanly examine geometrical confinement of the liquid atoms by the rigid atoms of the wall^{49,50}. At this interface, layer formation in the liquid part is seen; indeed layer formation is significantly more pronounced in these solid-liquid interface simulations at $T = 400$ K than in the free surface simulations, and there is considerable layer formation even at the high temperature of 800 K.

It is of course also interesting to consider the arrangement of the liquid atoms parallel to the wall, in particular to see if it is influenced by the fixed 2D order of the wall. In Fig. 9

the pair correlation functions, and bond angle and nearest neighbor distributions for our model solid-liquid interface are shown. For the two simulations, we present pair correlation functions, and bond angle and nearest neighbor distributions for the layer of liquid atoms closest to the wall, and averaged over inner liquid layers defined as lying within (i). the maximum-maximum regions, and (ii). the minimum-minimum regions.

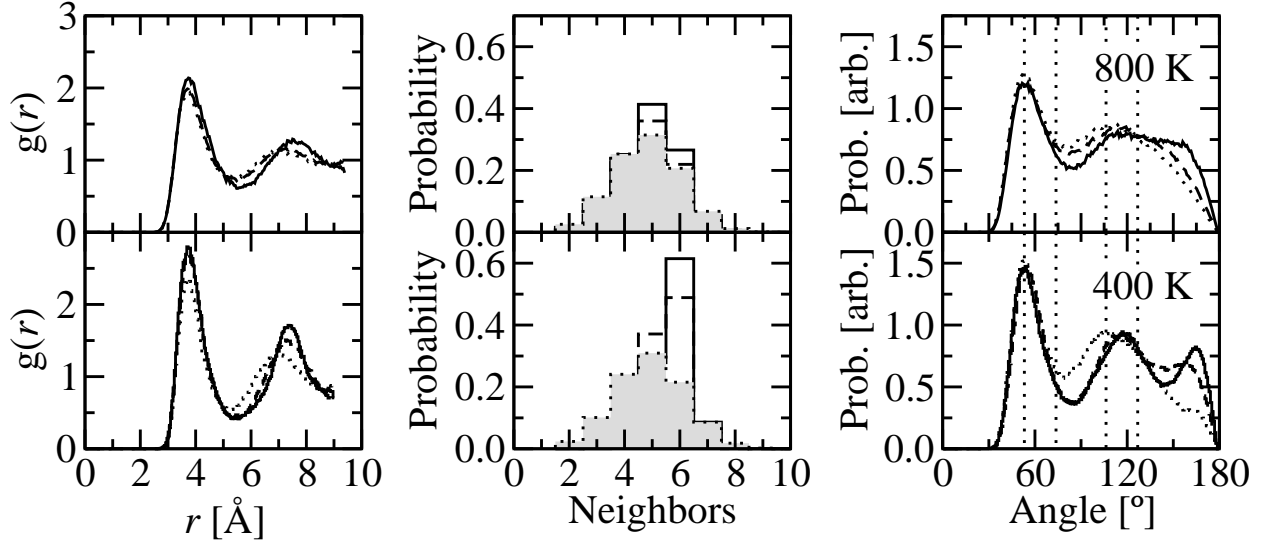


FIG. 9: Pair correlation functions (left panels), nearest neighbor distributions (center panels) and bond angle distributions (right panels) for solid-liquid interface model. The upper panels refer to $T = 800$ K, the lower panels to $T = 400$ K. The solid curves refer to the layers of liquid atoms nearest to the wall, the dashed curves to averages over the inner layers lying between *minima* in the density profiles, the dotted curves to averages over the inner layers lying between *maxima* in the density profiles. The vertical dotted lines in the bond angle distribution plots indicate the bond angles within the distorted hexagonal fixed layer.

The bond angle distributions for the solid-liquid interface show noticeable differences between the liquid layer closest to the fixed layer and those in the inner region. The quasi-hexagonal (that is, slightly distorted) arrangement of the atoms in the fixed layer means the bond angles in it are not exactly those of the perfect hexagonal arrangement (60° , 120° and 180°), but instead: 53.1° , 73.7° , 106.3° , 126.9° and 180° . In the liquid layers nearest the fixed layer, the bond angle distributions indicate a favoring of angles near 120° and an increase in weight at angles toward 180° ; the same type of effect of which we saw some hint in the free surface simulations. The shift in weight towards higher angles is enhanced as the

temperature is lowered. This indicates that the 2D order in the liquid layers adjacent to the fixed layer is influenced by the structure of that layer: upon moving further from the fixed layer into the liquid, the degree of order is reduced, meaning the 2D order becomes less definite. Also as the temperature is lowered, the disorder in the liquid part is lowered, meaning the influence of the 2D order of the fixed layer is greater.

The average coordination numbers in the various liquid layers obtained by averaging the nearest neighbor distributions are shown in Table III. In the liquid layer adjacent to the fixed layer, the coordination is close to the value of six that the atoms within the fixed layer have, especially at $T = 400$ K; it decreases in the inner layers, and also when the temperature is increased to 800 K. The coordination numbers in the minimum-minimum layers are larger than in the maximum-maximum layers, which is consistent with the idea of the atoms being ordered *within* the layers defined by the density peaks, where there are more atoms.

T [K]	First liquid layer	Inner: min-min	Inner: max-max
400	5.8	5.5	4.9
800	5.0	4.9	4.8

TABLE III: Coordination numbers n_c obtained by averaging the nearest neighbor distributions from the classical simulations shown in Fig. 9.

The pair correlation functions for the fixed layer simulations shown in Fig. 9 display small differences in the position of the first peak between the liquid layer adjacent to the fixed layer and the inner layers, but there is a definite shift in the position of the second peak to larger values in the first liquid layer compared to the inner layers. This is the same type of behavior we saw in comparing the pair correlation functions for the surface layers and the inner layers in the density functional theory free surface simulations. At $T = 400$ K, the first minimum (to the right of the first peak) is quite deep, and the first peak is higher in the liquid layer adjacent to the wall, which supports the idea that the 2D order in the fixed layer influences the liquid layer adjacent to it (this deepening of the minimum and increase in the height of the maximum is a signature of the correlation function in the fixed layer, that consists of a series of spikes at the nearest neighbor, second nearest neighbor, etc. distances): what we see in the liquid layer adjacent to the fixed layer is a smeared

version of this.

Now we attempt to rationalize the 2D ordering behavior suggested by our simulations. The nearest neighbor and bond angle distributions given above, suggesting predominantly 5-fold and 6-fold coordinated atomic arrangements, can be explained by considering an ordering reminiscent of the hexatic phase to be present at the surface.

Firstly we take the most probable spacing between atoms in the surface layer indicated by the pair correlation functions, 3.8 \AA . We consider a close-packed hexagonal arrangement of atoms with this spacing (this will contain 25 atoms for perfect hexagonal arrangement), and then remove a couple of these atoms and introduce some disorder into the arrangement (as indicated schematically in Fig. 10). This cartoon is intended to give a qualitative indication of what the atomic arrangement might look like; the nearest neighbor distance is used as a guide to the size of the atoms. In this way, we estimate that the number of atoms in such a layer should be $\sim 24 - 25^{49,50}$, and the average coordination number would be a bit less than 6.

For slabs consisting of around 160 atoms formed into quasi-close-packed layers, a total of 7 layers would be expected. This is in agreement with the numbers of layers present in the slab simulations as indicated by the density profiles⁴⁹.

Fig. 5 of Ref. 51 shows 2D density plots calculated at the surfaces – that is, at the positions of the surface peaks in the density profiles – for the (001) *ab initio* slab simulations discussed in this paper. Inspection of those plots shows that there is considerable structure in the surface layers, with regions consistent with five- and six-fold coordinated ordering, in accordance with the bond angle and nearest neighbor distributions presented above, and our schematic picture of distorted hexagonal ordering in the surface layer.

III. CONCLUSIONS

The data we have presented in this paper suggest a weak tendency toward two-dimensional atomic ordering within the layers formed at liquid metal surfaces, especially the surface layer. Nearest neighbor distributions indicate predominantly a mixture 5-fold and 6-fold coordinated sites at the surface (though there are notable fractions of 4-fold coordinated sites), with the average coordination within the surface layers being just over 5. The fraction of 4-fold coordinated sites decreased as the temperature is lowered, while the

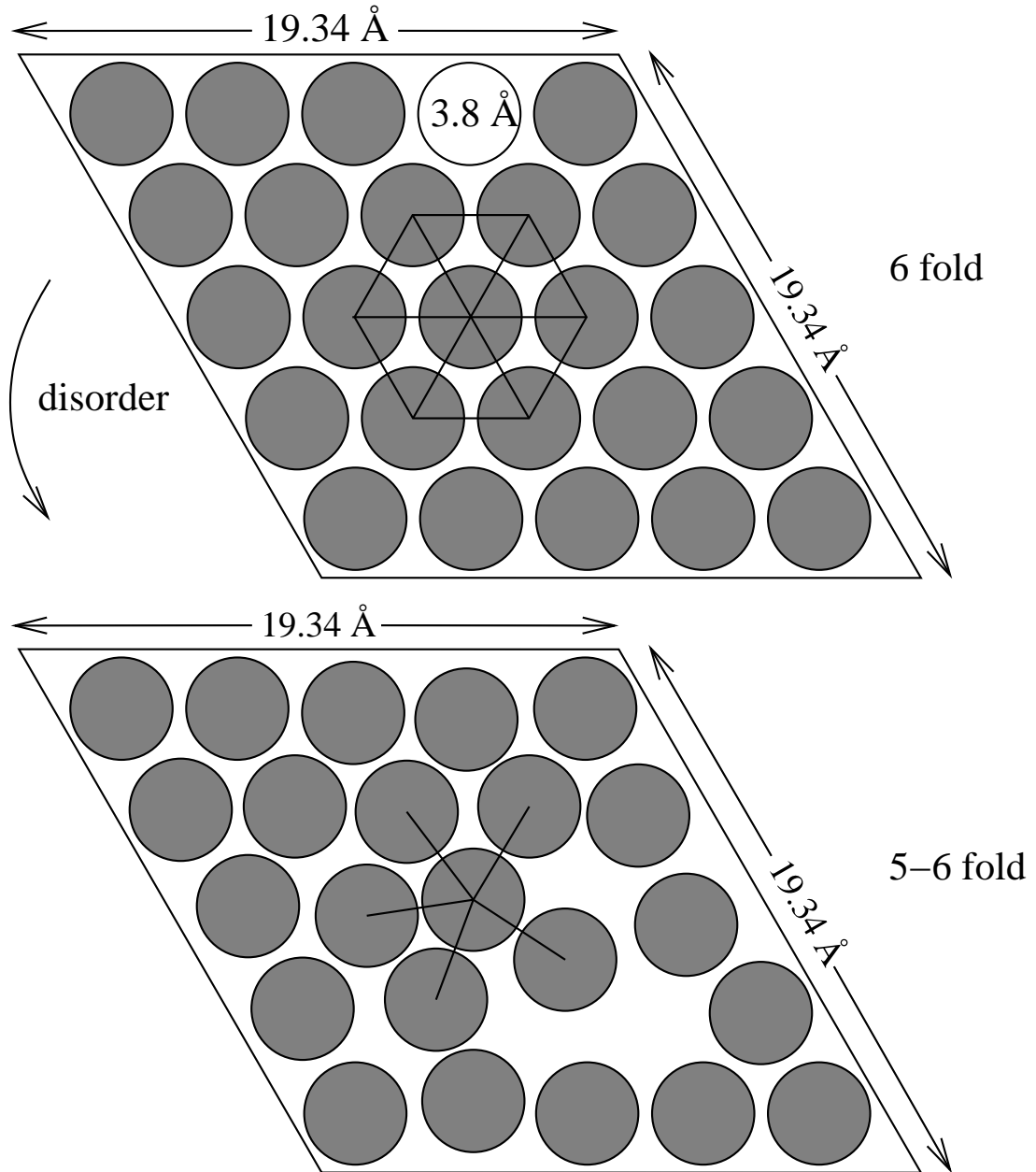


FIG. 10: Schematic illustration of taking a hexagonally close-packed set of atoms (upper part), removing a couple of them, and introducing some disorder into the positions of those remaining, to obtain a distorted hexagonal ordering (lower part). The cell is of the (111) shape and the cell dimensions are those appropriate for $T = 500$ K.

fractions of 5- and 6-fold coordinated sites increase at the surface. Bond angle distributions indicate increased tendency toward the three bond angles of a hexagonally close-packed two-

dimensional structure, at the surface. We have rationalized this data from the *ab initio* MD simulations by considering a slight disordering of a hexagonally-ordered two-dimensional structure.

The classical and *ab initio* DFT free liquid surface simulations we have described show broadly similar results in that both types of simulation produce a layered surface density, and are consistent with the results of orbital-free density functional theory simulations^{13,14,15}. There are however differences between the *ab initio* free surface density profiles and the classical and orbital-free DFT results in that the *ab initio* densities show outermost peaks larger than or of comparable height to the subsequent peaks away from the surface, whereas the classical and orbital-free simulations consistently show surface peaks of lower height than the subsequent peaks. The analysis of the experimental results^{20,26,29,31,32,33,34,35,39,46,47} gives density profiles with surface peaks with heights greater than those of the subsequent peaks.

Acknowledgments

BGW thanks the New Zealand Foundation for Research Science and Technology and the Cambridge Overseas Trust for studentships. NM acknowledges computational support from NSF DMR-0414849 and PNNL EMSL-UP-9597.

* Electronic address: b.walker@irl.cri.nz

¹ Internet homepage of the Harvard X-Ray Group:

<http://www.liquids.deas.harvard.edu/>.

² The hexatic phase occurs when molecules are packed together like racked billiard balls, though not held together rigidly by bonds. The particles move about as in a liquid, and a freeze frame would show that there is no long-range order present. The average molecular coordination is 6 as in hexagonal ordering, though there is the occasional 5-fold coordinated atom, which will always be situated near one that is 7-fold coordinated. Additional information can be found at: <http://focus.aps.org/story/v10/st5>.

³ F. Celestini, F. Ercolessi, and E. Tosatti. *Phys. Rev. Lett.*, 78:3153, 1997.

- ⁴ E. Chacón, M. Reinaldo-Falagán, E. Velasco, and P. Tarazona. *Phys. Rev. Lett.*, 87:166101–1, 2001.
- ⁵ D. S. Chekmarev, M. Zhao, and S. A. Rice. *J. Chem. Phys.*, 109:768, 1998.
- ⁶ D. S. Chekmarev, M. Zhao, and S. A. Rice. *Phys. Rev. E*, 59:479, 1999.
- ⁷ M. P. D’Evelyn and S. A. Rice. *Phys. Rev. Lett.*, 47:1844, 1981.
- ⁸ M. P. D’Evelyn and S. A. Rice. *Discuss. Faraday Soc.*, 16:71, 1982.
- ⁹ M. P. D’Evelyn and S. A. Rice. *J. Chem. Phys.*, 78:5225, 1983.
- ¹⁰ M. P. D’Evelyn and S. A. Rice. *J. Chem. Phys.*, 78:5081, 1983.
- ¹¹ G. Fabricius, E. Artacho, D. Sánchez-Portal, P. Ordejón, D. A. Drabold, and J. M. Soler. *Phys. Rev. B*, 60:R16283, 1999.
- ¹² M. A. Gomez and S. A. Rice. *J. Chem. Phys.*, 101:8094, 1994.
- ¹³ D. J. González, L. E. González, and M. J. Stott. *Phys. Rev. Lett.*, 92:085501–1, 2004.
- ¹⁴ D. J. González, L. E. González, and M. J. Stott. *Phys. Rev. Lett.*, 94:077801–1, 2005.
- ¹⁵ D. J. González, L. E. González, and M. J. Stott. *Phys. Rev. B*, 74:014207, 2006.
- ¹⁶ J. Gryko and S. A. Rice. *J. Non. Cryst. Solids*, 61/62:703, 1984.
- ¹⁷ J. Gryko and S. A. Rice. *J. Chem. Phys.*, 80:6318, 1984.
- ¹⁸ J. G. Harris, J. Gryko, and S. A. Rice. *J. Chem. Phys.*, 87:3069, 1987.
- ¹⁹ S. Iarlorigi, P. Carnevali, F. Ercolessi, and E. Tosatti. *Surface Science*, 211/212:55, 1989.
- ²⁰ E. H. Kawamoto, S. Lee, P. S. Pershan, M. Deutsch, N. Maskil, and B. M. Ocko. *Phys. Rev. B*, 47:6847, 1993.
- ²¹ G. Kresse and J. Hafner. *Phys. Rev. B*, 47:558, 1993.
- ²² N. Lei, Z. Huang, and S. A. Rice. *J. Chem. Phys.*, 104:4802, 1996.
- ²³ N. Lei, Z. Huang, and S. A. Rice. *J. Chem. Phys.*, 105:9615, 1996.
- ²⁴ N. Lei, Z. Huang, and S. A. Rice. *J. Chem. Phys.*, 107:4051, 1997.
- ²⁵ B. C. Lu and S. A. Rice. *J. Chem. Phys.*, 68:5558, 1978.
- ²⁶ O. M. Magnussen, B. M. Ocko, M. J. Regan, K. Penanen, P. S. Pershan, and M. Deutsch. *Phys. Rev. Lett.*, 74:4444, 1995.
- ²⁷ N. Marzari. *Ab-initio Molecular Dynamics for Metallic Systems*. PhD thesis, University of Cambridge, 1996.
- ²⁸ N. Marzari, D. Vanderbilt, A. De Vita, and M. C. Payne. *Phys. Rev. Lett.*, 82:3296, 1999.
- ²⁹ E. Di Masi, H. Tostmann, B. M. Ocko, P. S. Pershan, and M. Deutsch. *Phys. Rev. B*, 58:R13419,

- 1998.
- ³⁰ C. Molteni, N. Marzari, M. C. Payne, and V. Heine. *Phys. Rev. Lett.*, 79:869, 1997.
- ³¹ M. J. Regan, E. H. Kawamoto, S. Lee, P. S. Pershan, N. Maskil, M. Deutsch, O. M. Magnussen, B. M. Ocko, and L. E. Berman. *Phys. Rev. Lett.*, 75:2498, 1995.
- ³² M. J. Regan, E. H. Kawamoto, S. Lee, P. S. Pershan, N. Maskil, M. Deutsch, O. M. Magnussen, B. M. Ocko, and L. E. Berman. *J. Non-Cryst. Solids*, 205-7:762, 1996.
- ³³ M. J. Regan, P. S. Pershan, O. M. Magnussen, B. M. Ocko, M. Deutsch, and L. E. Berman. *Phys. Rev. B*, 54:9730, 1996.
- ³⁴ M. J. Regan, P. S. Pershan, O. M. Magnussen, B. M. Ocko, M. Deutsch, and L. E. Berman. *Phys. Rev. B*, 55:15874, 1997.
- ³⁵ M. J. Regan, H. Tostmann, P. S. Pershan, O. M. Magnussen, E. DiMasi, B. M. Ocko, and M. Deutsch. *Phys. Rev. B*, 55:10786, 1997.
- ³⁶ H. Reichert, O. Klein, H. Dosch, M. Denk, V. Honkimäki, T. Lippmann, and G. Reiter. *Nature*, 408:839, 2000.
- ³⁷ S. A. Rice. *Proc. Natl. Acad. Sci. USA*, 84:4709, 1987.
- ³⁸ J. S. Rowlinson and B. Widom. *Molecular Theory of Capillarity*. Dover Publications Inc., New York, 2002.
- ³⁹ O. Shpyrko, P. Huber, A. Grigoriev, P. Pershan, B. Ocko, H. Tostmann, and M. Deutsch. *Phys. Rev. B*, 67:115405–1, 2003.
- ⁴⁰ O. G. Shpyrko, R. Streitl, V. S. K. Balagurusamy, A. Y. Grigoriev, M. Deutsch, B. M. Ocko, M. Meron, B. Lin, and P. S. Pershan. *Science*, 313:77, 2006.
- ⁴¹ D. Sluis, M. P. D’Evelyn, and S. A. Rice. *J. Chem. Phys.*, 78:1611, 1983.
- ⁴² F. Spaepen. *Nature*, 408:781, 2000.
- ⁴³ P. W. Sutter and E. A. Sutter. *Nature Materials*, 6:363, 2007.
- ⁴⁴ P. Tarazona, E. Chacón, M. Reinaldo-Falagán, and E. Velasco. *J. Chem. Phys.*, 117:3941, 2002.
- ⁴⁵ B. N. Thomas, S. W. Barton, F. Novak, and S. A. Rice. *J. Chem. Phys.*, 86:1036, 1987.
- ⁴⁶ H. Tostmann, E. Di Masi, P. S. Pershan, B. M. Ocko, O. G. Shpyrko, and M. Deutsch. *Phys. Rev. B*, 59:783, 1999.
- ⁴⁷ H. Tostmann, E. Di Masi, P. S. Pershan, B. M. Ocko, O. G. Shpyrko, and M. Deutsch. *Phys. Rev. B*, 61:7284, 2000.
- ⁴⁸ E. Valesco, P. Tarazona, M. Reinaldo-Falagán, and E. Chacón. *J. Chem. Phys.*, 117:10777, 2002.

- ⁴⁹ B. G. Walker, N. Marzari, and C. Molteni. *J. Chem. Phys.*, 124:174702, 2006.
- ⁵⁰ B. G. Walker, N. Marzari, and C. Molteni. *J. Phys: Condens. Matt.*, 18:L269, 2006.
- ⁵¹ B. G. Walker, C. Molteni, and N. Marzari. *J. Phys.: Condens. Matter*, 16:S2575, 2004.
- ⁵² M. Zhao, D. S. Chekmarev, Z. Cai, and S. A. Rice. *Phys. Rev. E*, 56:7033, 1997.
- ⁵³ M. Zhao, D. S. Chekmarev, and S. A. Rice. *J. Chem. Phys.*, 108:5055, 1998.
- ⁵⁴ M. Zhao, D. S. Chekmarev, and S. A. Rice. *J. Chem. Phys.*, 109:1959, 1998.
- ⁵⁵ M. Zhao and S. A. Rice. *J. Chem. Phys.*, 111:2181, 1999.